Journal of King Saud University – Science 33 (2021) 101225

Contents lists available at ScienceDirect

Journal of King Saud University – Science

journal homepage: www.sciencedirect.com

Original article

Biochemical composition, morphology and antimicrobial susceptibility pattern of *Corynebacterium pseudotuberculosis* biofilm

Mohamad Fakhri Yaacob [a], Aika Murata [b], Nurul Hidayah Mohamad Nor [c], Faez Firdaus Abdullah Jesse [d], Mohd Fakharul Zaman Raja Yahya [a,e,*]

[a] Faculty of Applied Sciences, Universiti Teknologi MARA Shah Alam, 40450 Shah Alam, Selangor, Malaysia
[b] National Institute of Technology, UBE College, 2-14-1 Tokiwadai, Ube, Japan
[c] National Centre of Particle Physics, University of Malaya, 50603 Kuala Lumpur, Malaysia
[d] Faculty of Veterinary Medicine, Universiti Putra Malaysia, 43400 UPM Serdang, Selangor, Malaysia
[e] Molecular Microbial Pathogenicity Research Group, Pharmaceutical and Life Sciences Community of Research, Universiti Teknologi MARA, Malaysia

ARTICLE INFO

Article history:
Received 12 August 2020
Revised 13 October 2020
Accepted 26 October 2020
Available online 4 November 2020

Keywords:
Biofilm
Extracellular polymeric substances
Corynebacterium pseudotuberculosis
Caseous lymphadenitis
Raman spectroscopy
Field emission scanning electron microscopy

ABSTRACT

Caseous lymphadenitis (CLA) is a ruminant disease caused by *Corynebacterium pseudotuberculosis,* a Gram-positive facultative intracellular pathogen. The present work was performed to investigate the biochemical composition, morphology and antimicrobial susceptibility pattern of *C. pseudotuberculosis* biofilm using Raman spectroscopy, field emission scanning electron microscopy (FESEM) and microplate biofilm assay respectively. Results showed that the 24-h-old biofilm was characterized by Raman spectral peaks at 615 cm^{-1} (CCC symmetric bend phenyl ring), 668 cm^{-1} (Valine) and 825 cm^{-1} (Ring breath Tyr.) whilst the 48-h-old and 72-h-old biofilms were characterized by Raman spectral peaks at 1400 cm^{-1} (COO— sym.), 1450 cm^{-1} (COO— sym.), 1581 cm^{-1} (Ring breath Trp.), 1650 cm^{-1} (COO— asym.) and 1725 cm^{-1} (C═O str.). Raman spectra also revealed the biochemical heterogeneity in *C. pseudotuberculosis* biofilm. FESEM images clearly showed the biofilm cells which were surrounded by the extracellular matrix. Treatment with nalidixic acid, streptomycin, tetracyclin, ethylenediaminetetraacetic acid (EDTA) and dimethyl sulfoxide (DMSO) significantly ($p < 0.05$) inhibited the viability of *C. pseudotuberculosis* biofilm. The present study suggests that the biochemical composition of *C. pseudotuberculosis* biofilm may vary across different developmental stages. Meanwhile, nalidixic acid, streptomycin, tetracyclin, EDTA and DMSO may be useful in the treatment of CLA.

1. Introduction

Caseous lymphadenitis (CLA) in small ruminants is caused by *Corynebacterium pseudotuberculosis,* a Gram-positive facultative intracellular pathogen. It is an easily transmitted infectious disease that commonly infects sheep and goats (Nascimento, 2020). The disease causes inflammation of the lymph node resulting in the formation of caseaous cheesy material in the nodes, abscess formation in superficial and internal lymph nodes as well as in internal organs (Cetinkaya et al., 2002). CLA cases have been reported by many countries such as Malaysia (Komala et al., 2008), Brazil (Guimarães et al., 2009), Egypt (Al-Gaabary et al., 2010), northern Norway (Hektoen, 2012), France and Spain (De La Fuente et al., 2017). The severity of CLA is expected to associate with biofilm formation of the causative organism.

Biofilm is a complex and structured microbial community that tends to attach to inert and living surfaces in the presence of

Abbreviations: CLA, Caseous lymphadenitis; *C. pseudotuberculosis*, *Corynebacterium pseudotuberculosis*; *S. typhimurium*, *Salmonella typhimurium*; FESEM, Field emission scanning electron microscope; h, Hours; Tyr, Tyrosine; sym, Symmetric; asym, Asymmetric; Trp, Tryptophan; str, Stretching; EDTA, Ethylenediaminetetraacetic acid; DMSO, Dimethyl sulfoxide; EPS, Extracellular polymeric substances; NIH, National Institutes of Health; VLSU, Veterinary Laboratory Service Unit; UPM, Universiti Putra Malaysia; ATCC, American type culture collection; OD, Optical density; nm, Nanometre; μm, Micrometre; mW, Milliwatt; Ω/cm, Ohm per centimetre; cm-1, Reciprocal centimetre; ml, Millilitre; °C, Degree Celsius; CCD, Charge-coupled device; s, Seconds; μg/ml, Microgram per millilitre; mM, Millimolar; μl, Microliter; IP, Intellectual property; NaOH, Sodium hydroxide; EtOH, Ethanol; MBEC, Minimum biofilm eradication concentration.

* Corresponding author.
E-mail address: fakharulzaman@uitm.edu.my (M.F.Z. Raja Yahya).

Peer review under responsibility of King Saud University.

Production and hosting by Elsevier

https://doi.org/10.1016/j.jksus.2020.10.022

extracellular polymeric substances (EPS) and causes a wide range of diseases. Bacteria within the biofilm become more resistant to antimicrobial treatment compared with planktonic counterparts because the bacterial community in the biofilm differs from its planktonic counterpart in the gene and protein expression patterns that typically results in distinct metabolic and antimicrobial resistance profiles (Giaouris et al., 2013). According to National Institutes of Health (NIH), among all microbial and chronic infections, 65% and 80%, respectively, are associated with the biofilm formation. Over the past few decades, many aspects of biofilms have been understood including basic life cycle, antimicrobial susceptibility pattern (Costerton et al., 1999), essential enzymes for biofilms (Yahya et al., 2014), biofilm heterogeneity (Yahya et al., 2017), chemical composition of EPS matrix (Costerton et al., 1999; Yahya et al., 2018) and whole-cell proteome expression (Giaouris et al., 2013; Zawawi et al., 2020).

Since the last few years, previous works have addressed the important genes for vaccination and the protein interaction networks in *C. pseudotuberculosis*. Hassan et al. (2014) adopted a novel integrative strategy combining substractive proteomics and modelomics. They successfully identified four essential and non-homologous proteins as potential vaccine targets. On the other hand, Folador et al. (2016) identified 181 essential proteins, among which 41 are non-host homologous from the inferred protein interaction networks. However, until now, there is still a lack of experimental data on *C. pseudotuberculosis* biofilm. Thus, the present work was performed to determine the biochemical composition of *C. pseudotuberculosis* biofilm using Raman spectroscopy. Biofilm morphology and biofilm susceptibility towards antimicrobials were investigated using field emission scanning electron microscopy (FESEM) and microplate biofilm assay respectively.

2. Materials and methods

2.1. Chemicals and antibiotics

The following commercially available antibiotics and chemicals were used herein: streptomycin (Sigma, USA), tetracyclin (Sigma, USA), nalidixic acid (Sigma, USA), ethylenediaminetetraacetic acid (Sigma, USA), dimethyl sulfoxide (Merck, Germany), ethanol (Merck, Germany), sodium hydroxide (Sigma, USA), sodium chloride (Sigma, USA), formaldehyde (Merck, Germany), hydrochloric acid (AJAX Chemicals), hydrogen fluoride (Merck, Germany), hydrogen peroxide (Merck, Germany), ammonium hydroxide (Merck, Germany), crystal violet (Sigma, USA) and resazurin (Sigma, USA).

2.2. Test microorganisms

C. pseudotuberculosis clinical isolate was obtained from Veterinary Laboratory Service Unit (VLSU), Department of Veterinary Pathology and Microbiology, Faculty of Veterinary Medicine, Universiti Putra Malaysia (UPM) while *Salmonella typhimurium* ATCC 14028 was obtained from Microbiology Laboratory, Faculty of Applied Sciences, Universiti Teknologi MARA Shah Alam. Both bacterial species were grown in nutrient broth (Difco Laboratories, USA) and incubated at 37 °C. Prior to biofilm assay, the bacterial inocula were adjusted to optical density (OD) of 0.7 at 600 nm.

2.3. Substrate

P-type Crystal Silicon (111) (Sigma, USA) with thickness of 625 ± 25 μm and 0–10 Ω/cm resistivity was used as a substrate. The substrate was cleaned using deionized water in order to remove dust and external particles on the surface of the substrate. The substrate was then immersed in H_2O:H_2O_2:HCl (with ratio of 6:1:1) solution for 10 m to remove the metallic and microbiological contaminants. In order to remove the organic residues and oxide layer, the substrates were immersed in H_2O:H_2O_2:NH_4OH (ratio 5:1:1) and H_2O:HF (with ratio of 10:1) solutions for 5 m for each solutions. Deionized water was used to rinse the samples after immersed in each solution. Finally, substrates were purge with N_2 gas to clean and dry the surface.

2.4. Microplate biofilm assay for spectroscopic and microscopic characterization

C. pseudotuberculosis biofilm was grown in 6-well microplate. Overnight inoculum (4 ml) was added into the microplate wells. Then, a volume of 1 ml of fresh nutrient medium was added. For spectroscopic and microscopic experiments, the sterile silicon substrate and glass cover slip were introduced into the biofilm assay with the surface of interest facing upward, respectively. The microplate was incubated overnight at 37 °C. Then, the silicon substrate and glass cover slip were removed from the microplate and rinsed with phosphate-buffered saline twice.

2.5. Raman spectroscopy

Raman spectra of biofilm were obtained using Renishaw InVia Raman microscope (Wotton-under-Edge, UK) with a charge-coupled device (CCD) detector and a diffraction grating of 1200 lines/mm. An argon ion laser with excitation wavelength and laser power of 514 nm and 10 mW respectively were used. The measurement was carried out by 100% laser power and 40 s exposure time. Scanning range was limited from 500 to 3200 cm^{-1}. Before measurement, the single crystalline silicone with 520 cm^{-1} Raman shift was used as calibration.

2.6. Field emission scanning electron microscopy

The morphology of *C. pseudotuberculosis* biofilm was studied using field emission scanning electron microscope (FESEM) (Hitachi, Japan). The biofilm on the glass cover slip was fixed in 4% formaldehyde at 4 °C for 3 h, rinsed with sterile distilled water thrice and dehydrated (once in 25%, 50%, 75% and twice in 100% of ethanol each for 10 m). The slide was air dried overnight and observed at 5000x magnification using FESEM.

2.7. Pellicle assay

C. pseudotuberculosis and *S. typhimurium* were grown in sterile test tubes. After incubation at 37 °C for 24 h, nutrient medium was discarded. The pellicle fractions were rinsed with sterile distilled water twice, heat-fixed at 60 °C for 30 m and stained with 0.5% crystal violet for 10 m. Then, the pellicle fractions were distained with sterile distilled water gently. The pellicle formation was inspected visually.

2.8. Antibiofilm screening assay

The susceptibility of *C. pseudotuberculosis* biofilm towards antimicrobials was evaluated using a range of veterinary antibiotics and common chemicals in 96-wells microplate. A stock of 0.02% resazurin was prepared and stored at 4 °C in the dark. Antibiotic solutions were prepared in distilled water to the concentration of 100 μg/ml, 50 μg/ml, 25 μg/ml, 12.5 μg/ml, 6.25 μg/ml and 3.12 μg/ml. Sodium hydroxide and Ethylenediaminetetraacetic acid (EDTA) solutions were prepared at 500 mM, 250 mM, 125 mM, 62,5mM, 31.3 mM and 15.6 mM while dimethyl sulfoxide (DMSO) and ethanol solutions were prepared at 50%, 25%, 12.5%, 6.25%, 3.13% and 1.56%. Overnight inocula (200 μl) were added into

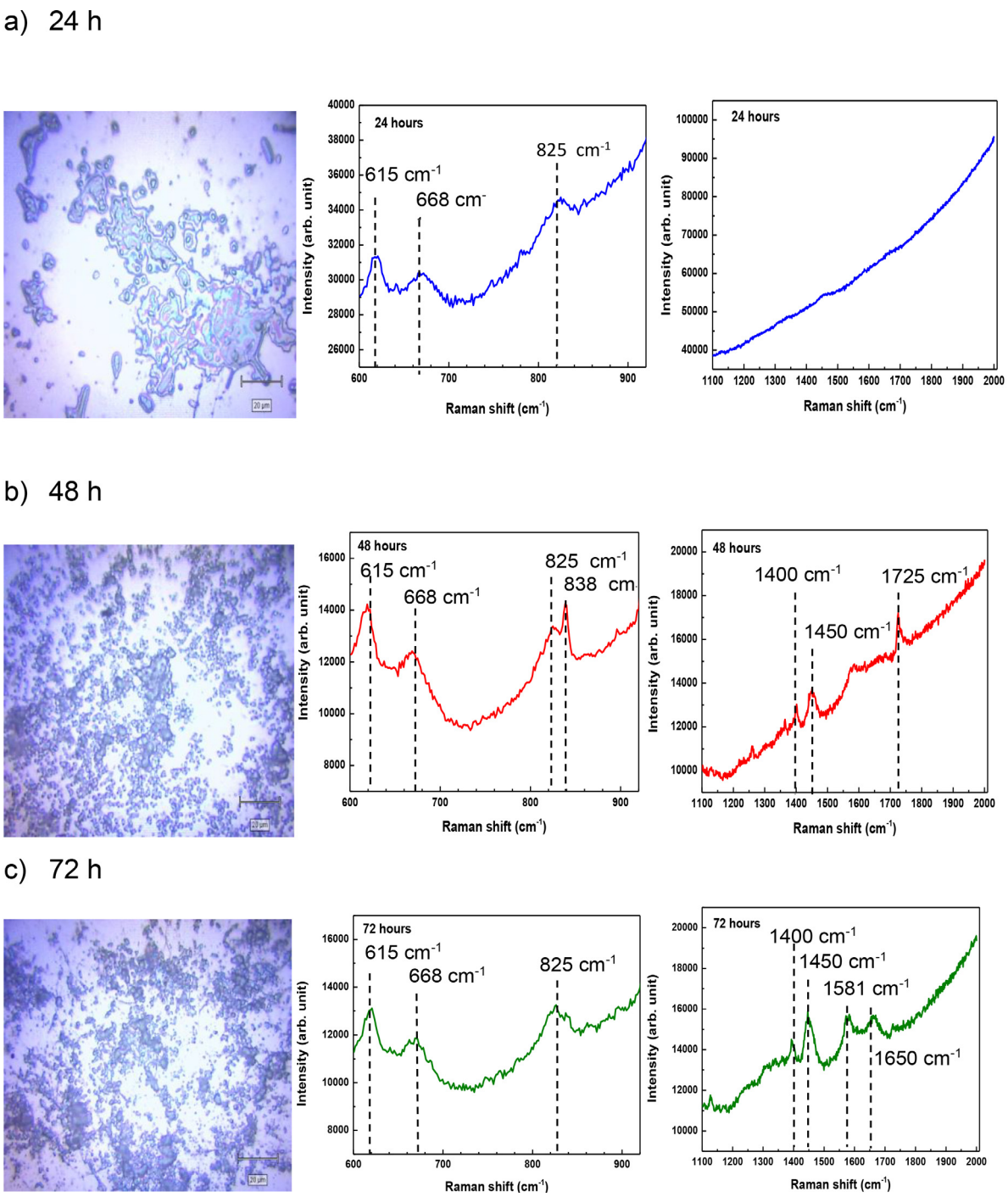

Fig. 1. Microscopic images at 100x magnification and the corresponding averaged spectra of *C. pseudotuberculosis* biofilm. a) 24 h-old biofilm; b) 48 h-old biofilm and c) 72-h biofilm. Spectral regions that commonly show organic molecules in biofilms: 600–900 cm^{-1}; 1100–2000 cm^{-1}. Functional groups: 615 cm^{-1} (CCC symmetric bend phenyl ring), 668 cm^{-1} (Valine), 825 cm^{-1} (Ring breath Tyr), 838 cm^{-1} (phosphodiester symmetric str.), 1400 cm^{-1} (COO— sym.), 1450 cm^{-1} (COO— sym.), 1581 cm^{-1} (Ring breath Trp.), 1650 cm^{-1} (COO— asym.) and 1725 cm^{-1} (C=O str.).

the microplate wells. Then, a volume of 50 μl of test solutions were added. Equal volume of fresh broth and intellectual property (IP)-protected antibiofilm cocktail were also added as negative and positive controls, respectively. The microplates were incubated overnight at 37 °C. On the following day, the medium was discarded whilst the biofilm fractions were rinsed with distilled water twice and heat-fixed at 60 °C for 30 min. The biofilm fractions were suspended in 220 μl of phosphate-buffered saline and 30 μl of 0.02% resazurin was added to the wells. The microplate was incubated for at least 3 h at 37 °C and analyzed using microplate reader (ThermoFisher Scientific, USA) for measuring absorbance at 570 nm.

2.9. Statistical analysis

All data from antibiofilm screening assay were expressed as mean ± standard deviation with n = 3. Independent *t* test was performed to determine the degree of significant difference between control and test groups whereby $p < 0.05$ was considered significant.

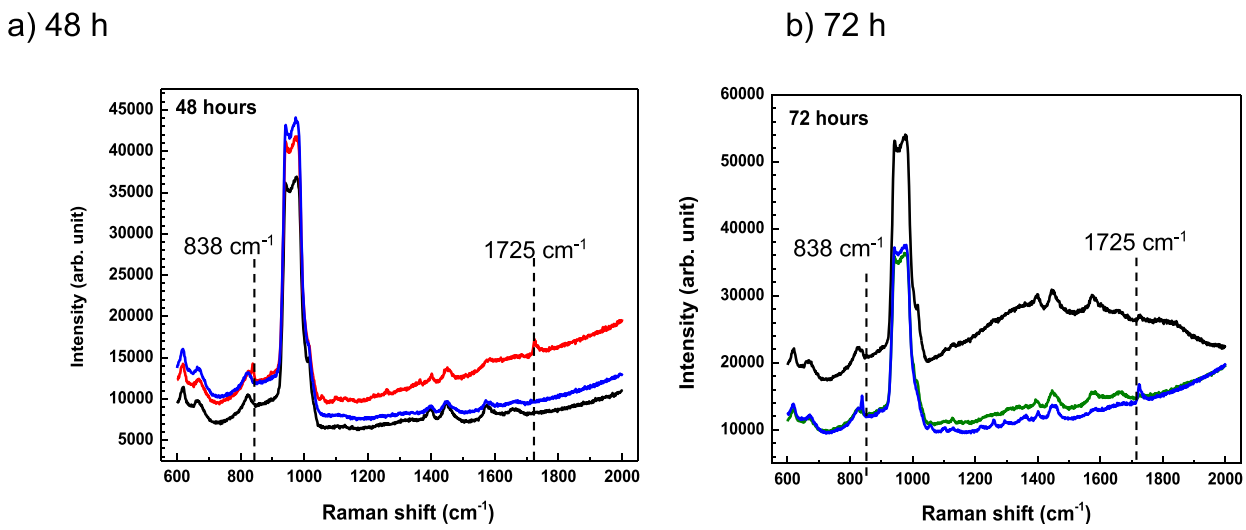

Fig. 2. Diverse Raman spectra within the specific stage of *C. pseudotuberculosis* biofilm. a) 48 h-old biofilm and b) 72 h-old biofilm. Functional groups: 838 cm^{-1} (phosphodiester symmetric str.) and 1725 cm^{-1} (C=O str.). Different colours in each panel indicate Raman spectra taken at three different locations within single biofilm samples.

3. Results

3.1. Differential Raman spectra of C. pseudotuberculosis biofilm across different growth stages

Fig. 1 shows microscopic images and averaged Raman spectra of *C. pseudotuberculosis* biofilm at 24 h, 48 h and 72 h. Microscopic images were compared with the corresponding averaged Raman spectra in order to determine the correlation between density and biochemical composition of *C. pseudotuberculosis* biofilm. Almost the entire surface of silicon substrate was covered by *C. pseudotuberculosis* cells at 48 h and 72 h, indicating the biofilm maturity. Across all stages, *C. pseudotuberculosis* biofilm showed Raman spectral peaks at 615 cm^{-1} (CCC symmetric bend phenyl ring), 668 cm^{-1} (Valine) and 825 cm^{-1} (Ring breath Tyr). The Raman spectral peaks at 1400 cm^{-1} (COO— sym.), 1450 cm^{-1} (COO— sym.), 1581 cm^{-1} (Ring breath Trp.), 1650 cm^{-1} (COO— asym.) and 1725 cm^{-1} (C=O str.) were observed to appear in both 48-h-old and 72-h-old biofilms, but not in 24-h-old biofilm. These five Raman spectral bands may specifically associate with the mature stage of *C. pseudotuberculosis* biofilm.

3.2. Heterogeneity of C. pseudotuberculosis biofilm at 48 h and 72 h

Fig. 2 shows the Raman spectra of *C. pseudotuberculosis* taken at three different locations of the *C. pseudotuberculosis* biofilm. Raman spectral peaks in the range 1000–9000 cm^{-1} indicated the silicon substrate. There were no differences in all Raman spectra of *C. pseudotuberculosis* at 24 h. However, inconsistent Raman spectral bands at 835 cm^{-1} (phosphodiester symmetric str.) and 1725 cm^{-1} (C=O str.) were observed in 48 h-old biofilm and 72 h-old biofilm, showing the biochemical heterogeneity.

3.3. Morphology of C. pseudotuberculosis biofilm

Fig. 3 shows the morphology of *C. pseudotuberculosis* biofilm at a magnification of 5000x. Rod-shaped cells of *C. pseudotuberculosis* were clearly observed in the 24-h-old biofilm. There was only one layer of biofilm that was formed on the surface. The biofilm cells were also encapsulated in a fibrous extracellular matrix.

3.4. Pellicle formation at air–liquid interface

The pellicle formation was compared between *C. pseudotuberculosis* biofilm and *S. typhimurium* biofilm. Fig. 4 shows *C. pseudotuberculosis* pellicle biofilm at air–liquid interface. It was found that *C. pseudotuberculosis* biofilm formed an intact pellicle similar to that formed by *S. typhimurium* biofilm.

3.5. Inhibitory action of antibiotics against C. pseudotuberculosis biofilm

The biofilm susceptibility towards antibiotics was compared between *C. pseudotuberculosis* biofilm and *S. typhimurium* biofilm. Fig. 5 shows the antibiofilm activities of antibiotics. Four test

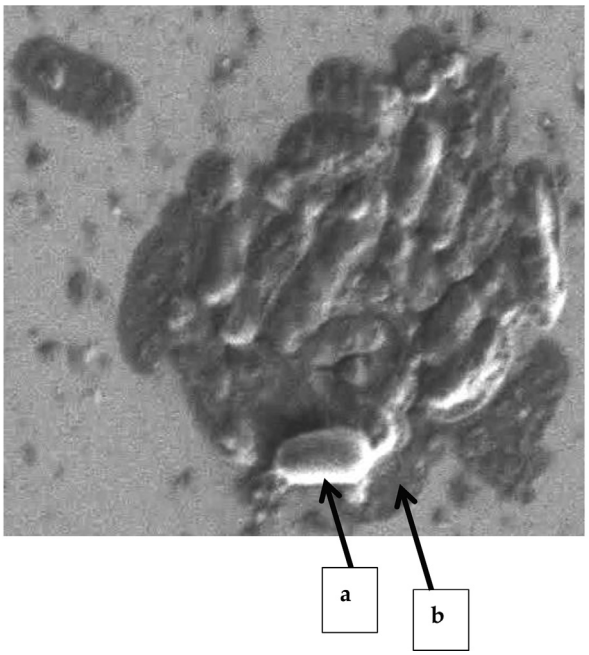

Fig. 3. FESEM image of *C. pseudotuberculosis* biofilm at 5000x magnification. a) Biofilm cells; b) Extracellular matrix.

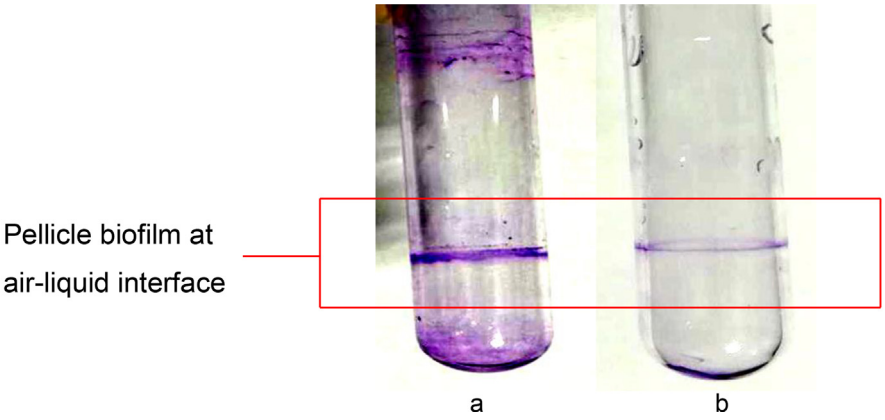

Fig. 4. Formation of pellicle biofilm at air–liquid interface. a) *S. typhimurium*; b) *C. pseudotuberculosis*. Adequate staining with 0.5% crystal violet, 25% methanol was achieved after 5 min.

concentrations of streptomycin (3.12 μg/ml, 12.5 μg/ml, 25 μg/ml, 100 μg/ml) significantly ($p < 0.05$) inhibited *C. pseudotuberculosis* biofilm. The same effect was also observed in *S. typhimurium* biofilm. Three test concentrations of tetracyclin (3 μg/ml, 12.5 μg/ml, 50 μg/ml) significantly ($p < 0.05$) inhibited *C. pseudotuberculosis* biofilm but not *S. typhimurium* biofilm. Two test concentrations of nalidixic acid (25 μg/ml, 50 μg/ml) significantly ($p < 0.05$) inhibited *C. pseudotuberculosis* and *S. typhimurium* biofilms while 12.5 μg/ml nalidixic acid significantly ($p < 0.05$) inhibited *C. pseudotuberculosis* biofilm but not *S. typhimurium* biofilm.

3.6. Inhibitory action of common chemicals against C. pseudotuberculosis biofilm

The biofilm susceptibility towards common chemicals was compared between *C. pseudotuberculosis* biofilm and *S. typhimurium* biofilm. Fig. 6 shows antibiofilm activities of common chemicals. Two test concentrations of EDTA (250 mM and 500 mM) significantly ($p < 0.05$) inhibited *C. pseudotuberculosis* and *S. typhimurium* biofilms. All test concentrations of DMSO (1.56%, 3.13%, 6.25%, 12.5%, 25%, 50%) significantly ($p < 0.05$) inhibited *C. pseudotuberculosis* biofilm but not *S. typhimurium* biofilm. NaOH and ethanol did not show any significant inhibitory actions against *C. pseudotuberculosis* biofilm and *S. typhimurium* biofilm.

4. Discussion

Proteinaceous components are important for all stages of biofilm formation. They play crucial roles in initial attachment to surface, stabilization of the biofilm matrix via interactions with exopolysaccharide and nucleic acid components, and development of three-dimensional biofilm architectures. The present study showed the presence of Raman spectral peaks associated with protein groups (615 cm^{-1}, 668 cm^{-1}, 828 cm^{-1} and 1581 cm^{-1}) in *C. pseudotuberculosis* biofilm (Fig. 1). Raman spectral peak at 1581 cm^{-1} (Trp. proteins) may represent a component of extracellular matrix of *C. pseudotuberculosis* biofilm (Ivleva et al., 2009).

Multiple lines of evidences have shown that lipids are present on the plasma membrane and extracellular matrix which are important for the architectural stability of the microbial complex. In most cases, planktonic and biofilm cells exhibit different profiles of sterol and sphingolipid. Herein, Raman spectral peaks at 668 cm^{-1} (CN+(CH3)3 str., lipids) and 1650 cm^{-1} (C═C and C═O, lipids) were found to be present in *C. pseudotuberculosis* biofilm (Fig. 1). The Raman spectral peak at 668 cm^{-1} has been shown to be present in *Pseudomonas aeruginosa* biofilm (Jung et al., 2014).

It has been established that the dense extracellular matrix surrounding mature biofilms is composed primarily of glycoproteins and carbohydrates along with lipids and nucleic acids. Carbohydrates function in providing structure to biofilms, allowing stratification of the bacterial community and establishing gradients of nutrients and waste products. Raman spectral peaks associated with carbohydrate group (1400 cm^{-1}, 1450 cm^{-1}, 1650 cm^{-1} and 1725 cm^{-1}) were identified in the present study (Fig. 1). These Raman spectral peaks may also represent components of extracellular matrix of *C. pseudotuberculosis* biofilm (Ivleva et al., 2009).

Mature biofilms from both clinical and environmental settings have been extensively investigated due to its harmful impacts and antimicrobial resistance phenotype. In most experiments, the 48-h-old biofilm and older ones are considered as mature biofilms. Herein, the mature *C. pseudotuberculosis* biofilms were characterized by the Raman spectral peaks associated with proteins, carbohydrates and lipids groups (Fig. 1). This result may indicate the domination of extracellular matrix of the mature *C. pseudotuberculosis* biofilm by high composition of protein fraction and relatively lower composition of saturated fatty acids and polysaccharides (Ramirez-Mora et al., 2019).

Physiological heterogeneity in the biofilm is due to the multilayer microbial communities and three dimensional structures that are established on the surface. In the present study, the heterogeneity in *C. pseudotuberculosis* biofilm based on altered Raman spectra was observed at 48 h and 72 h (Fig. 2). Spectra taken from different positions within single biofilm colonies could reveal the formation of more than one layer in the colonies (Kelestemur et al., 2018). Thus, changes in Raman spectral features are useful to explain heterogeneity in different developmental stages of *C. pseudotuberculosis* biofilm (Sandt et al., 2007).

FESEM analysis is useful for biofilm study because it provides information on the size, shape, production of extracellular matrix and localization within the biofilm of single bacteria. In the present study, FESEM images showed that the extracellular matrix surrounded the *C. pseudotuberculosis* biofilm cells and attached them to surface (Fig. 3). It is believed that extracellular matrix may play an important role in establishing *C. pseudotuberculosis* biofilm on surfaces (Combrouse et al., 2013; Ivleva et al., 2009; Jung et al., 2014; Ramirez-Mora et al., 2019).

Biofilm tends to form pellicle at air–liquid interface in aerobic environment. The pellicle gives a more cloudy appearance to the culture than planktonic population. Glucose-rich, cellulose-like polymer is essential for the formation of a pellicle at the air–liquid

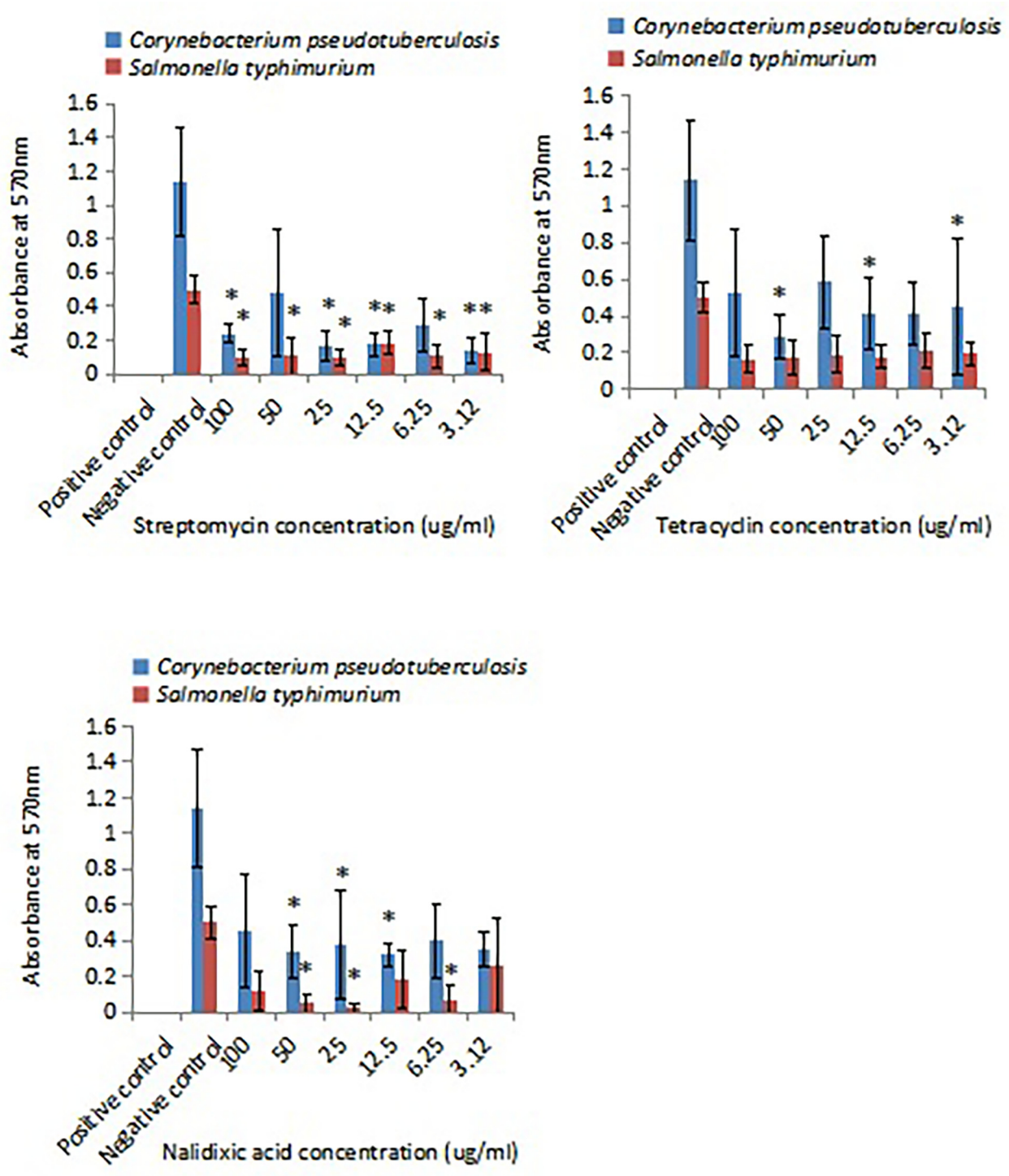

Fig. 5. Inhibitory effects of antibiotics on *C. pseudotuberculosis* biofilm and *S. typhimurium* biofilm. Positive control: overnight inocula added with IP-protected antibiofilm cocktail; negative control: overnight inocula added with fresh broth. Each bar represents mean ± standard deviation. Significant differences ($p < 0.05$) when compared with control group are shown by *.

interface. In the present study, *C. pseudotuberculosis* biofilm successfully formed the pellicle at air–liquid interface like *S. typhimurium* biofilm (Fig. 4). According to Jolly (1965), the pellicle formation contributes to the pathogenesis of *Corynebacterium ovis*. Thus, the pellicle formation observed herein may also play role in the pathogenesis of *C. pseudotuberculosis.*

Streptomycin controls the bacterial infection by inhibiting the binding of formyl-methionyl-tRNA to the 30S subunit during protein synthesis. In the present study, streptomycin effectively inhibited *C. pseudotuberculosis* biofilm (Fig. 5). This finding contradicts Olson et al. (2002) that demonstrated the resistance of *C. pseudotuberculosis* biofilm against streptomycin with the minimum biofilm eradication concentration (MBEC) values greater than 256 μg/ml. The disparity in this case is probably due to different growth medium used in the respective experiment whereby nutrient broth was used in the present study whilst tryptic soy broth supplemented

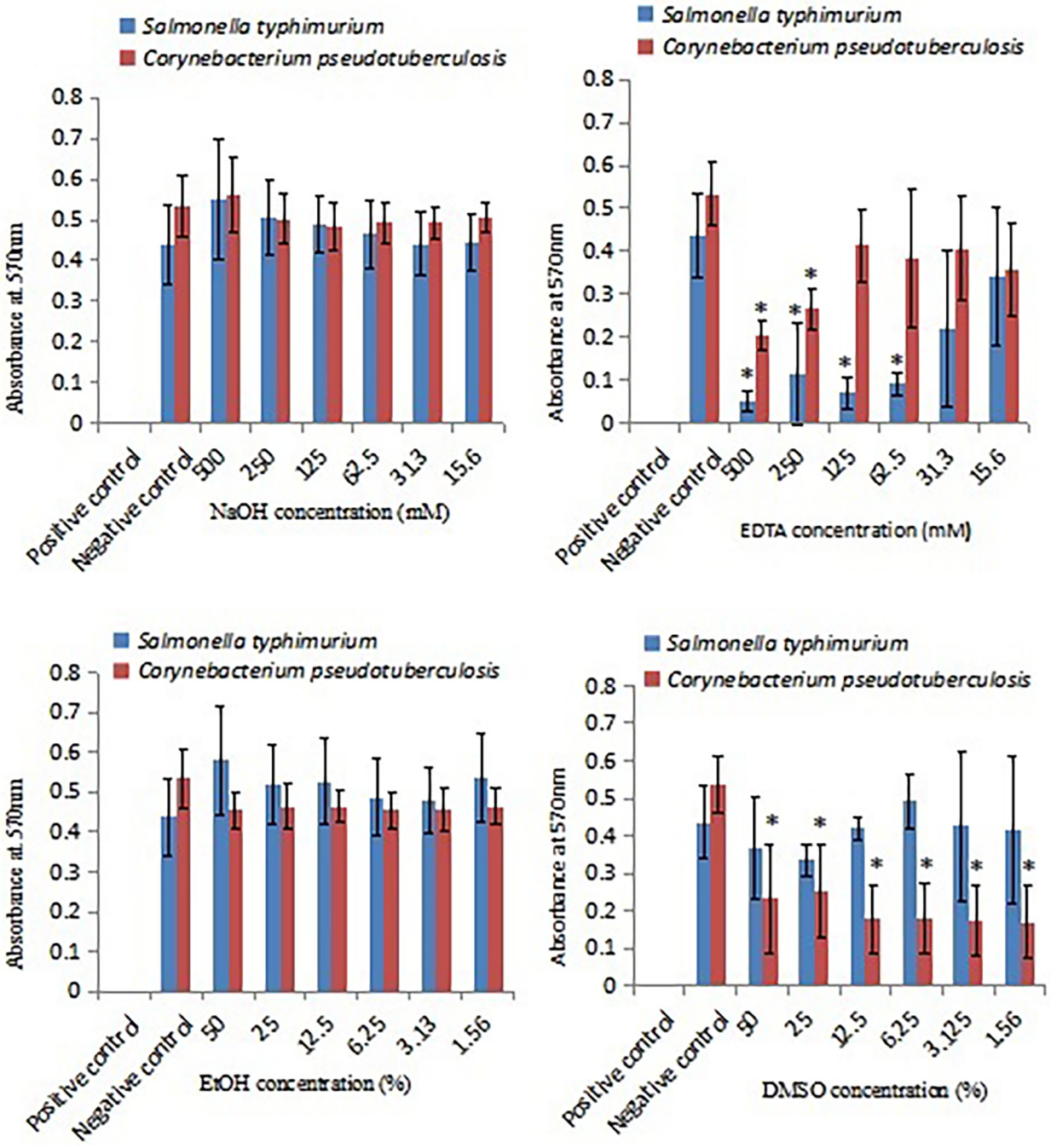

Fig. 6. Effect of common chemicals on *C. pseudotuberculosis* biofilm and *S. typhimurium* biofilm. Positive control: overnight inocula added with IP-protected antibiofilm cocktail; negative control: overnight inocula added with fresh broth. Each bar represents mean ± standard deviation. Significant differences ($p < 0.05$) when compared with control group are shown by *.

with fetal bovine serum was used in the study performed by Olson et al. (2002). The present study used only nutrient broth because *C. pseudotuberculosis* biofilm was being compared with a veterinary model pathogen namely *S. typhimurium* to investigate the pellicle formation and antibiofilm activity.

Inhibition of bacterial growth by DMSO is known to involve membrane perturbation. The present study revealed the inhibitory action of DMSO against *C. pseudotuberculosis* biofilm (Fig. 6). Inhibition of *C. pseudotuberculosis* biofilm by four disinfectants namely iodine, chlorhexidine, chlorine and quaternary ammonia has previously been reported (Sá et al., 2013). The present finding provides the first evidence for antibiofilm activity of DMSO against *C. pseudotuberculosis* and also suggests the potential use of DMSO as a surface disinfectant to control microbial surface attachment (Siddiqui et al., 2016).

Based on the significantly effective test concentrations, discrepancies in antibiofilm susceptibility pattern between *C. pseudotuberculosis* biofilm and *S. typhimurium* biofilm were observed. In Fig. 5, *C. pseudotuberculosis* biofilm was less susceptible to streptomycin and more susceptible to tetracyclin, as compared with *S. typhimurium* biofilm. On the other hand, *C. pseudotuberculosis* biofilm was less susceptible to EDTA and more susceptible to DMSO, as compared with *S. typhimurium* biofilm (Fig. 6). These discrepancies remain not well understood, however, the possible explanations

are possibly due to the presence of outer membrane proteins in Gram-negative pathogen (Rollauer et al., 2015) and species-dependent antimicrobial effects (Fernandes et al., 2020).

5. Conclusions

We have demonstrated the biochemical composition and morphology of *C. pseudotuberculosis* biofilm. The pellicle formation of *C. pseudotuberculosis* biofilm is similar to that of *S. typhimurium* biofilm while the antibiofilm susceptibility pattern of *C. pseudotuberculosis* is slightly different from that of *S. typhimurium*. To our knowledge, the present study represents the first effort to extensively characterize the biofilm formation by *C. pseudotuberculosis* that may mediate the persistence of CLA in small ruminants. A detailed investigation on how these antimicrobials could inhibit *C. pseudotuberculosis* biofilm at gene and protein expression levels need further attention.

Declaration of Competing Interest

The authors declare that they have no known competing financial interests or personal relationships that could have appeared to influence the work reported in this paper.

Acknowledgement

The authors are grateful to Faculty of Science, University of Malaya Kuala Lumpur, Malaysia for providing technical advice on Raman spectroscopy and FESEM.

Funding

This research was funded by Malaysian Ministry of Higher Education under a research grant, 600-IRMI/FRGS 5/3 (417/2019).

References

Al-Gaabary, M.H., Osman, S.A., Ahmed, M.S., Oreiby, A.F., 2010. Abattoir survey on caseous lymphadenitis in sheep and goats in Tanta, Egypt. Small Rum. Res. 94, 117–124. https://doi.org/10.1016/j.smallrumres.2010.07.011.

Cetinkaya, B., Karahan, M., Atil, E., Kalin, R., De Baere, T., 2002. Vaneechoutte, M. Identification of *Corynebacterium pseudotuberculosis* isolates from sheep and goats by PCR. Vet. Microbiol. 88, 75–83.

Combrouse, T., Sadovskaya, I., Faille, C., Kol, O., Guerardel, Y., Midelet-Bourdin, G., 2013. Quantification of the extracellular matrix of the *Listeria monocytogenes* biofilms of different phylogenic lineages with optimization of culture conditions. J. Appl. Microbiol. 114, 1120–1131. https://doi.org/10.1111/jam.12127.

Costerton, J.W., Stewart, P.S., Greenberg, E.P., 1999. Bacterial Biofilms: a common cause of persistent infections. Science 284, 1318–1322. https://doi.org/10.1126/science.284.5418.1318.

De La Fuente, R., De Las Heras, M., Torrijos, C., Diez de Tejada, P., Pérez-Sancho, M., Carrión, F.J., Orden, J.A., Dominguez-Bernal, G., 2017. Short communication: isolation frequency of bacteria causing lymphadenitis and abscesses in small ruminants in central Spain. Small Rum. Res. 154, 5–8. https://doi.org/10.1016/j.smallrumres.2017.06.022.

Fernandes, S., Gomes, I.B., Simões, M., 2020. Antimicrobial activity of glycolic acid and glyoxal against *Bacillus cereus* and *Pseudomonas fluorescens*. Food Res. Int. 136.

Folador, E.L., de Carvalho, P.V., Silva, W.M., Ferreira, R.S., Silva, A., Gromiha, M., et al., 2016. In silico identification of essential proteins in *Corynebacterium pseudotuberculosis* based on protein-protein interaction networks. BMC Syst. Biol. 10, 103. https://doi.org/10.1186/s12918-016-0346-4.

Giaouris, E., Samoilis, G., Chorianopoulos, N., Ercolini, D., Nychas, G.J., 2013. Differential protein expression patterns between planktonic and biofilm cells of Salmonella enterica serovar Enteritidis PT4 on stainless steel surface. Int. J. Food Microbiol. 162, 105–113. https://doi.org/10.1016/j.ijfoodmicro.2012.12.023.

Guimarães, A.S., Seyffert, N., Bastos, B.L., Portela, R.W.D., Meyer, R., Carmo, F.B., Cruz, J.C.M., McCulloch, J.A., Lage, A.P., Heinemann, M.B., Miyoshi, A., Azevedo, V., Gouveia, A.M.G., 2009. Caseous lymphadenitis in sheep flocks of the state of Minas Gerais, Brazil: prevalence and management surveys. Small Rum. Res. 87, 86–91. https://doi.org/10.1016/j.smallrumres.2009.09.027.

Hassan, S.S., Tiwari, S., Guimarães, L.C., et al., 2014. Proteome scale comparative modeling for conserved drug and vaccine targets identification in *Corynebacterium pseudotuberculosis*. BMC Genomics 15.

Hektoen, L., 2012. An outbreak of caseous lymphadenitis in a Norwegian ram circle and attempts to eliminate the disease. Small Rum. Res. 106, 25–26. https://doi.org/10.1016/j.smallrumres.2012.04.015.

Ivleva, N.P., Wagner, M., Horn, H., Niessner, R., Haisch, C., 2009. Towards a nondestructive chemical characterization of biofilm matrix by Raman microscopy. Anal. Bioanal. Chem. 393, 197–206. https://doi.org/10.1007/s00216-008-2470-5.

Jolly, R.D., 1965. The pathogenic action of the exotoxin of *Corynebacterium ovis*. Comp. Path. 75, 417–431.

Jung, G.B., Nam, S.W., Choi, S., Lee, G., Park, H., 2014. Evaluation of antibiotic effects on *Pseudomonas aeruginosa* biofilm using Raman spectroscopy and multivariate analysis. Biomed. Opt. Express 5, 3238–3251.

Kelestemur, S., Avci, E., Culha, M., 2018. Raman and Surface-Enhanced Raman scattering for biofilm characterization. Chemosensors. 6 (5). https://doi.org/10.3390/chemosensors6010005.

Komala, T.S., Ramlan, M., Yeoh, N.N., Surayani, A.R., Sharifah Hamidah, S.M., 2008. A survey of caseous lymphadenitis in small ruminant farms from two districts in Perak, Malaysia – Kinta and Hilir Perak. Trop. Biomed. 25 (3), 196–201.

Nascimento, V.S.D.O., 2020. Can vaccinating sheep reduce the occurrence of caseous lymphadenitis?. Vet. Evidence 5.

Olson, M.E., Ceri, H., Morck, D.W., Buret, A.G., Read, R.R., 2002. Biofilm bacteria: formation and comparative susceptibility to antibiotics. Can. J. Vet. Res. 66, 86–92.

Ramirez-Mora, T., Dávila-Pérez, C., Torres-Méndez, F., Valle-Bourrouet, G., 2019. Raman spectroscopic characterization of endodontic biofilm matrices. J. Spectrosc. 1–7. https://doi.org/10.1155/2019/1307397.

Rollauer, S.E., Sooreshjani, M.A., Noinaj, N., Buchanan, S.K., 2015. Outer membrane protein biogenesis in Gram-negative bacteria. Philos. Trans. R. Soc. Lond. B Biol. Sci. 370 (1679), 20150023. https://doi.org/10.1098/rstb.2015.0023.

Sá, M.C.A., Veschi, J.L.A., Santos, G.B., Amanso, E.S., Oliveira, S.A.S., Mota, R.A., Veneroni-Gouveia, G., Costa, M.M., 2013. Activity of Disinfectants and Biofilm Production of *Corynebacterium pseudotuberculosis*. Pesquisa Vet. Bras. 33 (11), 1319–1324.

Sandt, C., Smith-Palmer, T., Pink, J., Brennan, L., Pink, D., 2007. Confocal Raman microspectroscopy as a tool for studying the chemical heterogeneities of biofilms in situ. J. Appl. Microbiol. 103, 1808–1820. https://doi.org/10.1111/j.1365-2672.2007.03413.x.

Siddiqui, R., Aqeel, Y., Khan, N.A., 2016. The use of dimethyl sulfoxide in contact lens disinfectants is a potential preventative strategy against contracting Acanthamoeba keratitis. Contact Lens Anterior Eye 39 (5), 389–393.

Yahya, M.F.Z.R., Alias, Z., Karsani, S.A., 2018. Antibiofilm activity and mode of action of DMSO alone and its combination with afatinib against Gram-negative pathogens. Folia Microbiol. 63, 23–30.

Yahya, M.F.Z.R., Alias, Z., Karsani, S.A., 2017. Subtractive protein profiling of *Salmonella typhimurium* biofilm treated with DMSO. Protein J. 36, 286–298.

Yahya, M.F.Z.R., Hamid, U.M.A., Norfatimah, M.Y., Kambol, R., 2014. In silico analysis of essential tricarboxylic acid cycle enzymes from biofilm-forming bacteria. Trends Bioinf. 7, 19–26.

Zawawi, W.M.A.W.M., Ibrahim, M.S.A., Rahmad, N., Hamid, U.M.A., Yahya, M.F.Z.R., 2020. Proteomic analysis of *Pseudomonas aeruginosa* treated with *Chromolaena odorata* extracts. Malaysia J. Microb. 16 (2), 124–133.